Proportional fuzzy feed-forward architecture control validation by wind tunnel tests of a morphing wing

Kammegne, Michel Joël tchatchueng; Botez, Ruxandra Mihaela; Grigorie, Lucian Teodor; Mamou, Mahmoud; Mébarki, Youssef

Publisher's version / Version de l'éditeur:
https://doi.org/10.1016/j.cja.2017.02.001
Chinese Journal of Aeronautics, 2017-02

Chinese Journal of Aeronautics, (2017), xxx(xx): xxx–xxx

Chinese Society of Aeronautics and Astronautics
& Beihang University

Chinese Journal of Aeronautics

cja@buaa.edu.cn
www.sciencedirect.com

Proportional fuzzy feed-forward architecture control validation by wind tunnel tests of a morphing wing

Michel Joël Tchatchueng Kammegne [a], Ruxandra Mihaela Botez [a,*], Lucian Teodor Grigorie [a,b], Mahmoud Mamou [c], Youssef Mébarki [c]

[a] *École de Technologie Supérieure, Montréal H3C1K3, Canada*
[b] *University of Craiova, Craiova, Dolj 200585, Romania*
[c] *Aerodynamics Laboratory, NRC Aerospace, National Research Council Canada, Ottawa K1A0R6, Canada*

Received 26 February 2016; revised 8 June 2016; accepted 29 November 2016

KEYWORDS

Actuators;
Control;
Experimental validation;
Morphing wing;
Wind tunnel test

Abstract In aircraft wing design, engineers aim to provide the best possible aerodynamic performance under cruise flight conditions in terms of lift-to-drag ratio. Conventional control surfaces such as flaps, ailerons, variable wing sweep and spoilers are used to trim the aircraft for other flight conditions. The appearance of the morphing wing concept launched a new challenge in the area of overall wing and aircraft performance improvement during different flight segments by locally altering the flow over the aircraft's wings. This paper describes the development and application of a control system for an actuation mechanism integrated in a new morphing wing structure. The controlled actuation system includes four similar miniature electromechanical actuators disposed in two parallel actuation lines. The experimental model of the morphing wing is based on a full-scale portion of an aircraft wing, which is equipped with an aileron. The upper surface of the wing is a flexible one, being closed to the wing tip; the flexible skin is made of light composite materials. The four actuators are controlled in unison to change the flexible upper surface to improve the flow quality on the upper surface by delaying or advancing the transition point from laminar to turbulent regime. The actuators transform the torque into vertical forces. Their bases are fixed on the wing ribs and their top link arms are attached to supporting plates fixed onto the flexible skin with screws. The actuators push or pull the flexible skin using the necessary torque until the desired vertical displacement of each actuator is achieved. The four vertical displacements of the actuators, correlated with the new shape of the wing, are provided by a database obtained through a preliminary aerodynamic optimization for specific flight conditions. The control system is designed to con-

* Corresponding author.
E-mail address: ruxandra.botez@etsmtl.ca (R.M. Botez).

Peer review under responsibility of Editorial Committee of CJA.

ELSEVIER Production and hosting by Elsevier

http://dx.doi.org/10.1016/j.cja.2017.02.001

trol the positions of the actuators in real time in order to obtain and to maintain the desired shape of the wing for a specified flight condition. The feasibility and effectiveness of the developed control system by use of a proportional fuzzy feed-forward methodology are demonstrated experimentally through bench and wind tunnel tests of the morphing wing model.

1. Introduction

In today's world, fuel burn reduction is a serious concern of all the players in the aerospace industry, not only because of the environmental impacts but also due to the economic aspects. The aerodynamic force component most responsible for fuel burn is the drag (weight also affects the drag and thus the fuel burn). Therefore, reducing the drag through the advanced design of aircraft wings is a way for aerodynamicists to develop advanced technologies towards green aviation.

Among the recent (feasible) technologies used to reduce the aerodynamic drag, researchers have evaluated the effectiveness of aircraft wing morphing.[1] Aimed at improvement of aerodynamic performance by increasing the lift-to-drag ratio, various scenarios to change the wing shape were tested: morphing the wing's upper surface or morphing its trailing or leading edges. From the morphing upper surface point of view, the target is to increase the laminar flow region over the aircraft wing by moving the laminar-to-turbulent transition point close to the wing airfoil trailing edge to obtain in this way a lower drag force.[2] Also, the inclusion of the morphing wing technology in the aircraft conception brings other advantages related to the possibilities to fly multiple types of missions as a multi-role aircraft and to create superior system capabilities, radically performing new maneuvers which would not be possible with conventional control surfaces.[3]

Several review papers have described the technologies to enable the morphing concept implementation in the aircraft industry, which have been tested to date.[1,4–6] The literature also reveals that numerous studies and research projects have been developed in the field by various entities such as universities, research institutes and industry. A collaborative research study explored a process to link analytical models and optimization tools with design methods to create energy-efficient lightweight wing/structure/actuator combinations for morphing aircraft wings.[7] At the University of Kentucky, an adaptive circular arc airfoil was used to control the aerodynamic flow[8], while researchers from the University of Tokyo realized a cross-sectional deformation of a laminar airfoil in order to obtain a drag reduction at the off-design angles of attack.[9] In Germany, at the Aerodynamics Institute, RWTH Aachen, an experimental model of an adaptive wing with an adjustable upper side over the entire chord was used in wind tunnel tests to show the possible improvement of the aerodynamic performance of wings at transonic speeds.[10]

Munday and Jacob used an adaptive actuator integrated in the wing structure. Experimental results showed an expansion of the laminar flow when the actuator was activated.[11] That research was extended with a conformal camber[12] and with an oscillating camber.[13] A similar experiment, with an oscillating camber, was performed by a multidisciplinary team, which investigated the low Reynolds number flow over an adaptive wing assembly.[14] They used a NACA4415 airfoil for their reference profile; the experimental model was equipped with piezoelectric actuators and a latex membrane to provide a flexible and smooth upper surface.

Some adaptive structure concepts for aeroelastic drag reduction and load alleviation were investigated by Miller in his Ph.D. thesis at the University of Manchester, UK,[15] wherein a rotating spar concept enabling the adaptive aeroelastic shape control of aircraft wings to reduce the drag was developed. That work also showed the application of an all-moving wing tip device with an adaptive torsional stiffness attachment as a passive load alleviation system.

Another method to change the camber line was introduced by Monner et al. at the DLR, Germany,[16] designing flexible Fowler flaps for an adaptive wing that allows both chordwise and spanwise differential camber variations during flight. Some active ribs flex both upper and lower skins. The same concept, but with segmented ribs, was studied by Poonsong in his Master's thesis at the University of Maryland.[17] His model used the ribs which are divided into six sections, each section being able to rotate approximately five degrees without causing significant discontinuity on the wing surface. The morphing wing actuation mechanism included two pneumatic actuators.

A different approach to adapt the structure shapes in wing morphing applications is based on the compliant mechanisms powered by a single input actuator. Such a system was built at the University of Michigan by Saggere and Kota to control a wing section.[18] The mechanism, in which the leading and trailing edges were reshaped by means of actuators, allowed the airfoil camber to change. A similar mechanism was designed, fabricated and tested in flight by a collaborative research team from FlexSys Inc., MI, USA and from Air Force Research Laboratory, Dayton, OH, USA, for a Mission Adaptive Wing.[19] Researchers from the University of Bristol, UK presented another morphing design for airfoils using compliant mechanisms.[20] Their design includes an early skeletal frame-type ground structure, in which the actuators were substituted to obtain a preset surface deflection.

Another method to adapt the structure's shapes, instead of using a mechatronic solution with hinges or linear bearings, is the "belt-rib" solution[21] presented by Campanile and Sachau from the DLR, Germany. The new "belt-rib" replaces the classical rib and allows camber changes within prescribed limits, while keeping the remaining parts' stiffness properties unaffected.

In addition to changes in the internal mechanism, various actuation mechanisms have been investigated. One of these methods is based on piezoelectric actuation. Wang et al., in the Smart Wing 2 program of DARPA, developed a high-rate large-deflection hingeless trailing edge control surface for a smart wing model.[22] The model consists of distributed

Please cite this article in press as: Kammegne MJT et al. Proportional fuzzy feed-forward architecture control validation by wind tunnel tests of a morphing wing, *Chin J Aeronaut* (2017), http://dx.doi.org/10.1016/j.cja.2017.02.001

piezoelectric stack actuators with and without hydraulic amplifiers and pumps, as well as aggressive tendon actuation. Researchers from the University of Kansas, USA and from Delft University of Technology, Netherlands presented a morphing wing model for UAVs using post-buckled pre-compressed (PBP) piezoelectric bender actuators.[23] Flight test showed that the roll control authority was increased by 38% and that the control derivatives were more than 3.7 times larger than conventional variants. Using PBP actuators also increased the actuation frequency, by an order of magnitude. Another morphing application, developed by researchers from Konkuk University, South Korea, used lightweight piezo-composite actuators (LIPCA) to actuate the trailing edges of biomimetic wing sections.[24] At the same university, another morphing wing application was developed for a small-scale expandable wing, which was separated into inner and outer wings as in a typical bird wing.[25] Under the inner wing section, two LIPCA actuators were attached and activated in the expanded wing state to modify the camber of the wing. Wind tunnel tests showed that the actuators' activation created significant additional lift. At Oregon State University, USA, the researchers investigated the use of piezoceramic actuators to control bio-inspired flexible wings.[26,27]

Two approaches for creating control surfaces with the support of microfiber composite (MFC) actuators were tested at California State University, USA.[28] In the first, flap-like structures were formed by bonding MFC actuators to each side of a metal substrate, while in the second, MFC actuators were bonded directly to the wing. Another actuation concept based on piezo-ceramic composite, known as macro-fiber composite actuators, was used by Bilgen et al. for adjusting the camber of wings in a series of studies.[29–31] Similar actuators were also used by Na and Kim at Seoul National University, South Korea in a study related to the nonlinear static analysis of smart wings which was aimed to determine the most efficient location for these actuators on smart wings.[32]

An Italian collaborative research project, with researchers from the University of Naples "Federico II", CIRA and Alenia Aeronautica, studied a morphing wing trailing edge concept by replacing the conventional flap device with a compliant rib structure actuated with shape memory alloy (SMA) wires.[33] A feasibility study to deflect a wing flap using SMA wires as actuators was undertaken by Nanyang Technological University, Singapore in collaboration with DSO National Laboratories, Singapore.[34] They designed and manufactured a wing prototype, and the entire system, consisting of a rib, SMA wires and the flap, was experimentally tested. At the University of Catania, Italy, SMA actuators were used to test the ability of a wing in order to modify its cross section by assuming the shape of two different airfoils, and to test the possibility of deflecting the profiles near the trailing edge in order to obtain hingeless control surfaces; two prototypes were realized by incorporating the variable airfoil and the hingeless aileron features respectively.[35] An Australian research team analysed the application of smart materials for adaptive airfoil control.[36] Further, the researchers designed, developed and tested a deformable wing model using ABS material for the skin. The deflection of the variable cambered wing was controlled by means of SMA actuators fixed underneath the wing skin, near the leading edge.[37]

With the final aim to obtain real-time optimized airfoils, our research team from the ETS in Montreal, Canada used the laminar-to-turbulent flow transition point as control variable in a morphing wing project funded by Consortium for Research and Innovation in Aerospace in Quebec (CRIAQ). Called CRIAQ 7.1, the project was developed in collaboration with Thales, Bombardier Aerospace, Ecole Polytechnique, and IAR-CNRC. The team developed a possibility to detect the transition point starting from the surface pressure distribution, the precision of the method being dictated by the density of the pressure sensors distributed along the airfoil chord.[38] The morphing wing experimental model was equipped with SMA actuators, actuating on two parallel lines. Two adaptive neuro-fuzzy controllers were designed in order to correlate each set of pressure differences with the deformations of airfoil produced by the two actuators; these pressure differences were calculated as differences between the pressures acting on calculated between the optimized and the reference airfoils.[39] A linear model of the heating and cooling phase from an SMA actuator was obtained in order to be used in the design of its controllers.[40] With the linear model, an on–off controller combined with a proportional–integral one was designed and experimentally tested in the wind tunnel.[41] Due to the strong nonlinear behavior of the SMA actuators, the team developed and experimentally evaluated a hybrid control system combining a fuzzy logic proportional-integral-derivative controller and a conventional on-off controller.[42,43] The final wind tunnel test of the morphing wing model using a real-time optimizer to close the control loop confirmed the project formulated hypothesis, proving the drag reduction as a consequence of the laminar flow expansion on the upper surface of the wing.[44,45]

In another small-scale morphing wing model developed by our research team, the actuation mechanism was based on some DC motors which rotated two eccentric shafts and morphed a flexible skin along two parallel actuation lines.[46] A position controller aiming to control the shape of the wing airfoil under different flow conditions was designed and tested in the Price-Païdoussis Wind Tunnel at the ETS in Montreal, Canada. As a supplementary validation, an analysis of the wind flow characteristics was performed; the pressure coefficients predicted by the numerical simulations were compared with those obtained from the experimental test.[47–50]

In this context, a new morphing wing international collaborative research project was initiated by industrial entities, research institutes and universities from Canada and Italy, and the project was developed on a full-scale portion of the wing of an aircraft, which was fully actuated using electrical actuators. The work disseminated here is a part of this project and describes the experimental results obtained with a variant of the control system developed to be used in the actuation of the flexible skin on the upper surface of the wing.

2. Morphing wing project specific issues

The present morphing wing research project may be considered as a continuation of the CRIAQ 7.1 project developed by our research team in the Research Laboratory in Active Controls, Avionics and Aeroservoelasticity (LARCASE) of the ETS in Montreal, Canada, in which SMA wires were used as actuators to morph the upper surface of a WTEA-TE1 wing profile. The multitude of specific issues solved in the previous project, came from the multidisciplinary integration in the

same experimental demonstrator model of strongly nonlinear actuators (SMA actuators) with optical and Kulite pressure sensors, real-time control algorithms for actuator positions, and real-time estimators and optimization algorithms for the laminar to turbulent transition point position. In the new multidisciplinary project, specialists participate by working from aerodynamics, aeroservoelasticity, mechanics, control and electrical engineering.

Called "Multi-Disciplinary Optimization" 505 (MDO 505), this new CRIAQ funded project seeks to realize fuel consumption optimization by applying morphing wing technology to an aircraft wing equipped with a morphing aileron. In this project, realized at the ETS in Montreal, Canada in collaboration with Thales, Bombardier Aerospace, Ecole Polytechnique, the Institute for Aerospace Research - National Research Council Canada (IAR-NRC), and with Italian researchers from Frederico II Naples University, CIRA and Alenia, a wing-aileron prototype (Fig. 1) is designed, tested and validated using wind tunnel tests at IAR-NRC. The aileron was a part of the original aircraft wing section, the optimization for morphing application being performed for the entire wing, including here the aileron. Unlike the previous morphing project (CRIAQ 7.1) of our research team, this project uses miniature electromechanical actuators instead of smart material actuators. The special challenges of the MDO 505 are: (A) to aerodynamically optimize a non-symmetrical wing by using numerical simulations; (B) to adapt the actuation mechanism of the flexible skin and its control system to fit into the very small space inside the wing; (C) to obtain a good reproducibility of the numerically optimized shape of the upper surface of the wing with the experimental one by using a minimum number of actuation points and a flexible skin attached on all four sides of the wing, and the attachment increases the rigidity of the skin and hampers the achievement of the upper surface reproducibility (experimental versus numerical). Moreover, all of these challenges need to be overcome by keeping the resistance structure of the wing segment in its original form.

Our research team first aimed to design and integrate in the experimental model a control system which was able to morph the wing according to the requirements imposed by the aerodynamic optimization results obtained for different flow cases given by various Mach numbers Ma, wing angles of attack α and aileron deflection angles δ. On the other hand, to evaluate the aerodynamic gains of the morphing wing model during the wind tunnel tests, the team had the task to develop a mechanism which was able to detect and visualize the airflow characteristics based on the data obtained from the pressure sensors installed on the upper surface of the morphing wing.

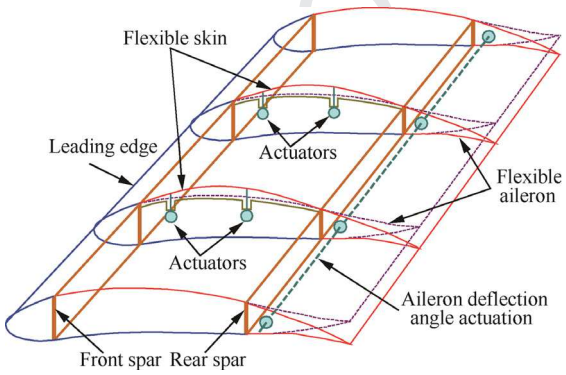

Fig. 1 Schematic structure of morphing wing.

The wing model was based on the dimensions of a full-scale wing tip structure, the span and chord of the model matching the dimensions found on a real aircraft wing tip, 1.5 m span and 1.5 m root chord with a taper ratio of 0.72. An optimization procedure was run by the aerodynamic team aiming to find the optimum airfoil shapes through local thickness modifications to improve the upper surface flow. The optimization was applied for several flight cases as combinations of Ma, α and δ. The adaptive upper surface is a flexible skin made from carbon fiber composite materials, which was positioned between 20% and 65% of the wing chord. The rigid structure, as well as the flexible skin, was specifically designed to meet aeronautical industry requirements. On the other hand, in the flexible skin design and optimization procedures, the match with the aerodynamically optimized upper surface shapes was considered as a determinant objective.

Once having established the structural constraints of the flexible skin and chosen the flight cases, the team resorted to the design of the actuation system, including here the actuation mechanism and the actuators. From technological constraints, it turned out that the actuation mechanism should include four actuators disposed on two actuation lines installed at 37% and 75% of the wing's span. Each actuator has the ability to operate independently from the others. On each actuation line, the actuators were positioned at 32% and 48% of the local wing chord.

The low space inside the wing required a direct actuation of the flexible skin, the in-house manufactured actuators being fixed with the lower part on the wing ribs and with the top on the flexible skin. To solidify the entire structure, the high grade industry steel and aluminum alloy materials were used to manufacture different internal structure elements.

The aerodynamic optimization procedure correlated with the actuator positions on the wing structure generated a database relating the actuator displacements and the optimized airfoils for different flight cases. Therefore, the actuators need to morph the upper surface of the wing until the desired displacements are achieved and an experimental airfoil approximating the optimized airfoil for a specified flight case is obtained. In order to achieve and maintain this airfoil shape even under the influence of external perturbations such as structural and aerodynamic loads, a robust control system should assist the actuation system. For each of the four actuation points, the actuation mechanism included a brushless direct current motor whose shaft was coupled to a gearing system with the other end attached and linked to a nut. Four linear variable differential transformers (LVDTs) were also used to measure the displacements of the four actuators (Fig. 2).

An in-house developed genetic algorithm was applied to the problem of airfoil upper-surface morphing. The problem objective was to search the optimum shapes for an airfoil through local thickness modifications with the aim of improving the upper surface flow and thus the aerodynamic performance of the airfoil. The vertical displacements for the actuators were determined from the genetic optimization of the wing airfoil. The optimization gave the displacement values for one pair of actuators situated at 37% of the wing span, while the displacements for the second pair of actuators were calculated as a linear dependence.

Please cite this article in press as: Kammegne MJT et al. Proportional fuzzy feed-forward architecture control validation by wind tunnel tests of a morphing wing, *Chin J Aeronaut* (2017), http://dx.doi.org/10.1016/j.cja.2017.02.001

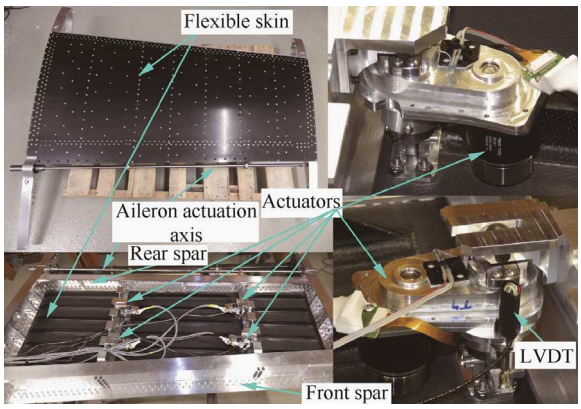

Fig. 2 Experimental model of morphing wing.

The obtained database of the optimized airfoils for different flight cases is firstly used to validate the morphing concept on this wing model for several flight cases as combinations of Ma, α and δ covering a flight envelope. Subsequently, the database may be used as "validated database of optimized airfoils" to generate another "optimized airfoils" through interpolation in the development of the embedded control system for a "real morphing wing" boarded on an aircraft, having as inputs the Mach number, the angle of attack and the aileron deflection angle provided by the onboard equipment.

In the next sections of the paper, the design and the experimental testing of the system controlling the positions of the four actuators are presented.

3. Controller design and bench test results

The control system of the experimental model was developed in two successive steps, generically called "open loop" and "closed loop". In the first architecture (open loop), the morphing wing system, and the aileron deflection angle are controlled, in the second architecture (closed loop), the open loop architecture is enclosed as an internal loop, the transition point position is controlled based on the information from the pressure sensors installed on the flexible skin and on the aileron upper surface. Therefore, the difference between the two architectures is the use of the information from the pressure sensors as feedback signal in the control algorithm. The presented work refers to the open loop architecture of the control system; it is based on the optimized airfoil database.

The actuation system was equipped with four identical actuators, requiring in this way the same position controllers. In the "open loop" architecture, the control system was experimentally tested in two situations: (A) on the bench, with no aerodynamic load, and (B) in the wind tunnel, with aerodynamic load corresponding to each optimized flight case.

For the wind tunnel tests, the inputs of the control loop are the vertical displacements of the actuators associated with the optimized airfoil which corresponds to the airflow conditions. This optimized airfoil is requested by the operator to be reproduced by the flexible skin, being selected from the computer database through the graphic interface list box and charged into the software. The software sends the vertical coordinates to the control loop at the actuators lines level, which required to reproduce the optimized airfoil. Therefore, for each flight case, the control system asks the actuators to morph the skin until the real vertical displacements $(dY_{1real}, dY_{2real}, dY_{3real}, dY_{4real})$ in the actuation points equal the vertical deflections $(dY_{1opt}, dY_{2opt}, dY_{3opt}, dY_{4opt})$ characterizing the differences between the optimized airfoil and the reference airfoil; the real vertical deflections (the control feedback) are measured by using the four LVDT sensors associated with each of the four actuators. The testing of the open loop architecture of the control system in the wind tunnel allows also the validation of the numerically obtained optimized airfoils through the real-time visualization of the transition point position based on the pressure sensors data.

On the other hand, the bench testing of the open loop architecture gave the opportunity to evaluate the level of reproducibility of the numerically optimized shape of the upper surface of the wing with the experimentally obtained one. To verify this reproducibility, the morphed wing was laser-scanned (Fig. 3) for each optimized airfoil in the database (for all optimized flight cases), and software results were compared with the numerical results in terms of skin shapes. To scan the surface, a portable scanner, called the 3D Handy Scan, was used, and targets were added on the skin surface. These targets are the white dots on the surface of the wing shown in Fig. 3. Targets were used when the object did not supply enough geometrical information to allow acquisition; thus, approximately 200 targets were used on the surface of the skin and ribs. Because a mirror-like surface (especially aluminum) prevented the laser from detecting the surface, a fine powder was applied on the wing. The targets were also needed to provide a reference for the scanner.

The second test of the open loop architecture, the wind tunnel test, allowed, on the other hand, the validation of the aerodynamic optimization of the system through the visualization of the transition point position for each optimized airfoil in the database (for all optimized flight cases). These visualizations are based on the information provided by the pressure sensors installed on the flexible skin. As a supplementary evaluation method for the transition point position in wind tunnel tests, an infrared visualization of the flow was performed by using the IAR-NRC experimental facility.

The bench test of the experimental model was performed in the LARCASE laboratory at the ETS in Montréal, Canada; the scheme of the experimental bench test used to validate the implemented controller in the open loop is presented in Fig. 4.

In this control mechanism, the real-time system converts the desired vertical positions in motor rotation units, asks the actuators to go to this positions (commands represented

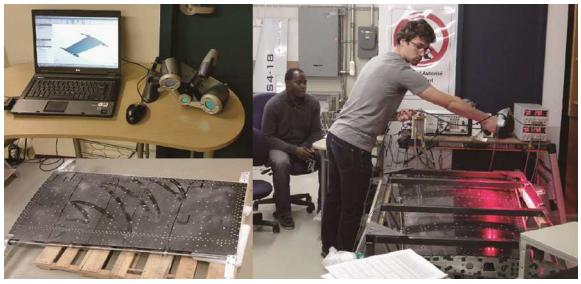

Fig. 3 Laser scanning of morphing wing during bench tests.

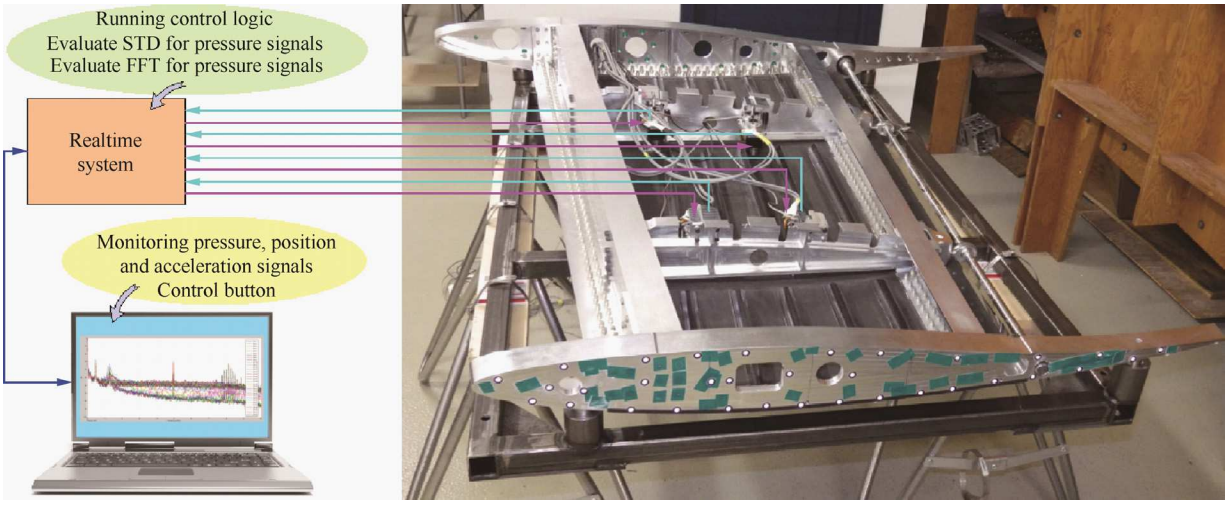

Fig. 4 Open loop control architecture in bench tests.

by the lines in magenta in Fig. 4), and obtains in the same time the feedback signals related to the real linear positions of the actuators by using the LVDT sensors data (signals represented by the cyan lines in Fig. 4). The controller's input and output are configured with the physical input/output of the target, so that when it is compiled and downloaded in the real-time target via the Ethernet cable (blue line with double arrows in Fig. 4), the data exchange can flow freely between the target and the hardware.

For the bench tests, our team conceived a graphic user interface (GUI) (Fig. 5) which helped the safe testing of various situations, not only from the control point of view but also from the flexible skin and actuator integration on the experimental model. Besides the simultaneous actuation, we followed the independent testing of the actuators in custom situations, evaluating in this way their power and at the same time the strength of the flexible skin in limit situations. Meanwhile, a communication was set between the GUI and the database relating the actuator displacements and the optimized airfoils for different flight cases, and thus the user was able to command the actuation for all these cases.

To develop the control system of the morphing wing actuators, a proportional fuzzy feedforward architecture was chosen[51,52] for each of the four controllers; its architecture is shown in Fig. 6, where each actuator is coupled to a controller.

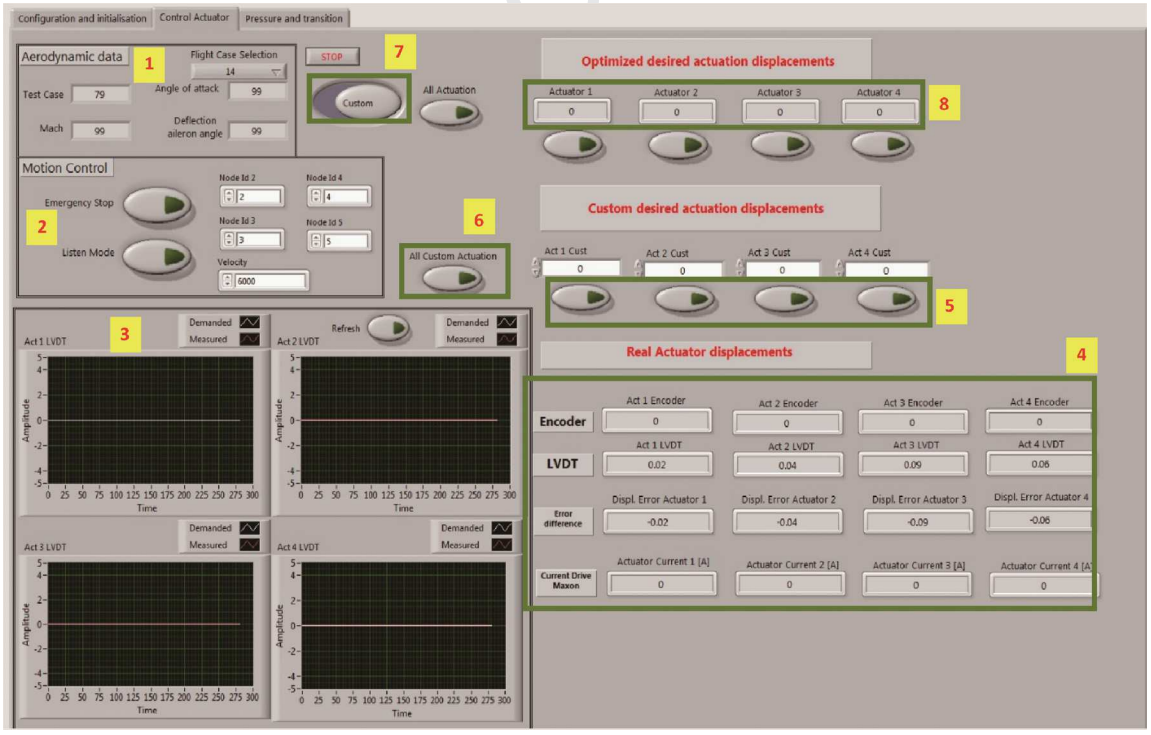

Fig. 5 Graphic user interface (GUI) developed for bench test of model.

The controller's input is the position error, and its output is the number of pulses required to reach the desired vertical position in millimeters. The controller's output is sent directly to the motor integrated in the actuator. The developed control system includes four similar controllers, and each one is associated to an actuator. The designed controllers were tuned based on knowledge obtained from the system behavior, the membership function parameters being determined by the trial and error method.

To design a fuzzy logic control system, four principal components must be considered: a fuzzifier, a fuzzy rule base, a fuzzy inference engine and a defuzzifier. In the fuzzifier stage, the crisp input e is transformed through the fuzzification into linguistic variables, which are further translated into linguistic concepts represented by fuzzy sets. Considering [−10, 10] interval as universe of discourse for the controller input, we chose eleven membership functions (MF) for it (Fig. 7). The considered shape for the inputs' membership functions was the triangular shape:

$$f_{\Delta}(x;a,b,c)=\begin{cases}0 & \text{if } x\leqslant a\\ \frac{x-a}{b-a} & \text{if } a<x<b\\ \frac{c-x}{c-b} & \text{if } b\leqslant x<c\\ 0 & \text{if } c\leqslant x\end{cases}=\max\left[\min\left(\frac{x-a}{b-a},\frac{c-x}{c-b}\right),\ 0\right] \quad (1)$$

where x is the independent variable on the universe, the parameters a and c locate at the feet of the triangle, and b gives its peak.

To define the rules, a Sugeno fuzzy model proposed by Takagi, Sugeno and Kang was selected. A Takagi, Sugeno and Kang fuzzy rule for a single-input-single-output system can be written in the following form:

$$\text{if } (x_1 \text{ is } A) \quad \text{then} \quad y=f(x_1) \quad (2)$$

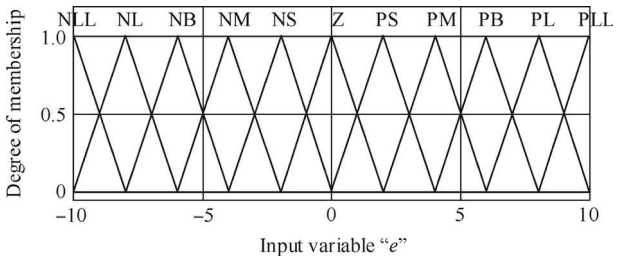

Fig. 7 Membership functions associated to input.

where A is fuzzy sets in the antecedent, $y=f(x_1)$ is a crisp function in the consequent, and $f(x_1)$ is a polynomial function. If f is a first-order polynomial, then the resulting fuzzy inference is called a first-order Sugeno fuzzy model, while if f is a constant, then it is a zero-order Sugeno fuzzy model. Considering a zero-order Sugeno fuzzy model, the membership functions of the output were chosen as constants in the [−10, 10] universe of discourse.

Starting from the inputs' and outputs' membership functions, a set of eleven inference rules were derived as shown in Fig. 8.

In the bench tests, the actuators were controlled simultaneously or independently to cover a large spectrum of interactions between them, the flexible skin and the rigid structure of the experimental model. All tests were performed in the laboratory conditions in the absence of the aerodynamic forces. Fig. 9 exposes the results obtained in a custom actuation situation when the four actuators where simultaneously triggered; two of these actuators have (Actuator 1 and Actuator 3) morphed the flexible skin downwards (negatively), while the other two actuators (Actuator 2 and Actuator 4) morphed the flexible skin upwards (positively). The actuators' responses were

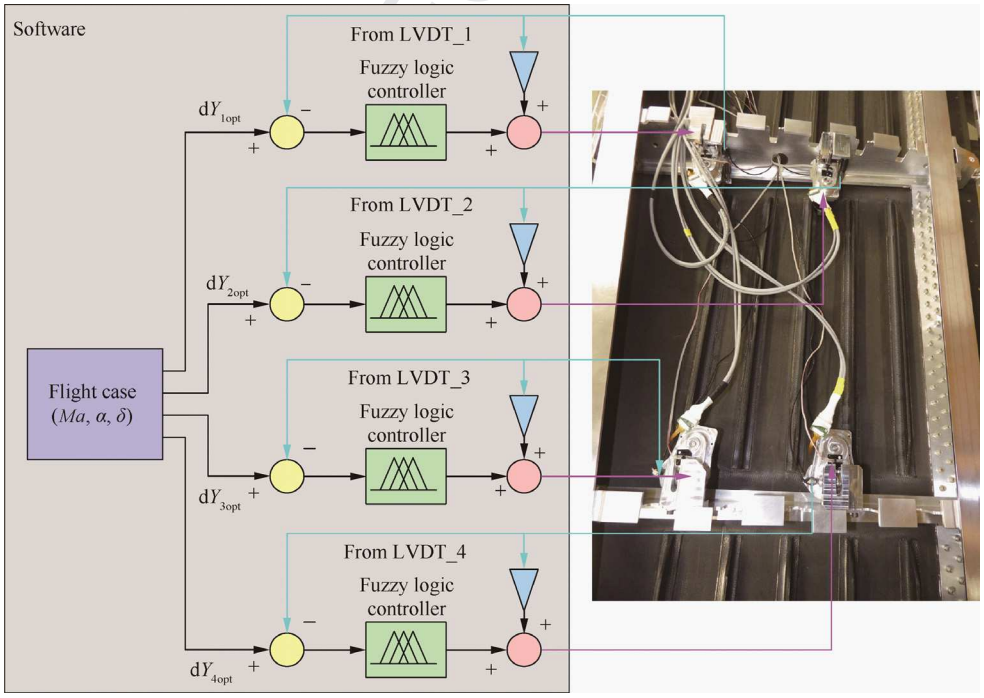

Fig. 6 Open loop control architecture of morphing wing model.

Please cite this article in press as: Kammegne MJT et al. Proportional fuzzy feed-forward architecture control validation by wind tunnel tests of a morphing wing, *Chin J Aeronaut* (2017), http://dx.doi.org/10.1016/j.cja.2017.02.001

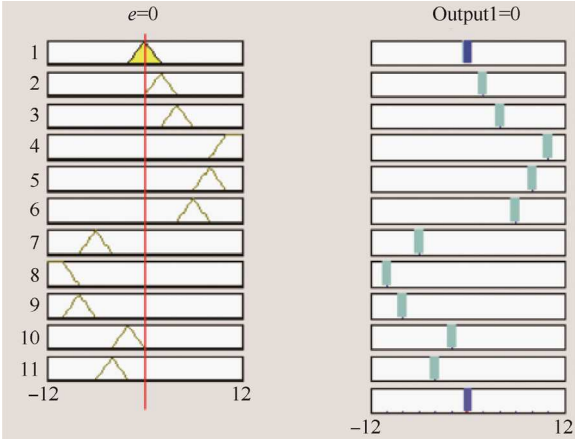

Fig. 8 Rules set in fuzzification process.

very good, although a slight time delay was observed, which was induced by the system inertia from both software processing and mechanical points of view. Similar results were noticed in all performed bench tests where Fig. 10 presented the responses of the actuators triggered independently for various repeated step signals as control inputs. From Figs. 9 and 10, it can also be easily observed that the very low level of the noise superposed on the linear variable differential transformer (LVDT) sensor signals. It is due to the filters integrated in the SCXI-1540 LVDT modules from National Instruments used as signal conditioners for LVDTs.

4. Experimental setup in wind tunnel

The schematic of the instrumented wing configuration for the wind tunnel tests is shown in Fig. 11. In the wind tunnel tests, under aerodynamic loads for a given optimal case, the miniature electrical actuators would push or pull the flexible skin using the necessary torque until the desired vertical displacement of each actuator is achieved. The skin displacement in each of the four actuation points is sensed by the linear positioning sensor (LVDT) mounted on the corresponding actuator. The acquired raw skin displacement is sent to the signal conditioner (SCXI), which supplies and processes the linear positioning sensor; it is indicated in Fig. 11 by the orange line. The output signal from the signal conditioner (the brown line in Fig. 11) is the actual skin displacement in millimeters. The encoder position needed to achieve the positioning control of the actuator is processed by the drive and read by the real-time system (PXI express); the encoder position is represented by the blue line.

The PXI express is a real-time machine using an integrated real-time operating system. The main advantages of that system are that it can be extended with other real-time systems and it is modular. Modular, in the sense that it is used here, means that different modules or cards can be inserted into the PXI express (PXI-e) chassis. For this project, the PXI-e chassis has been extended by five different modules. The first four modules (from left to right) are used to acquire the pressure sensors' signals, while the last module, which is a CAN open module, is used to communicate with the CAN network defined by the motor drive systems. Each of the pressure sen-

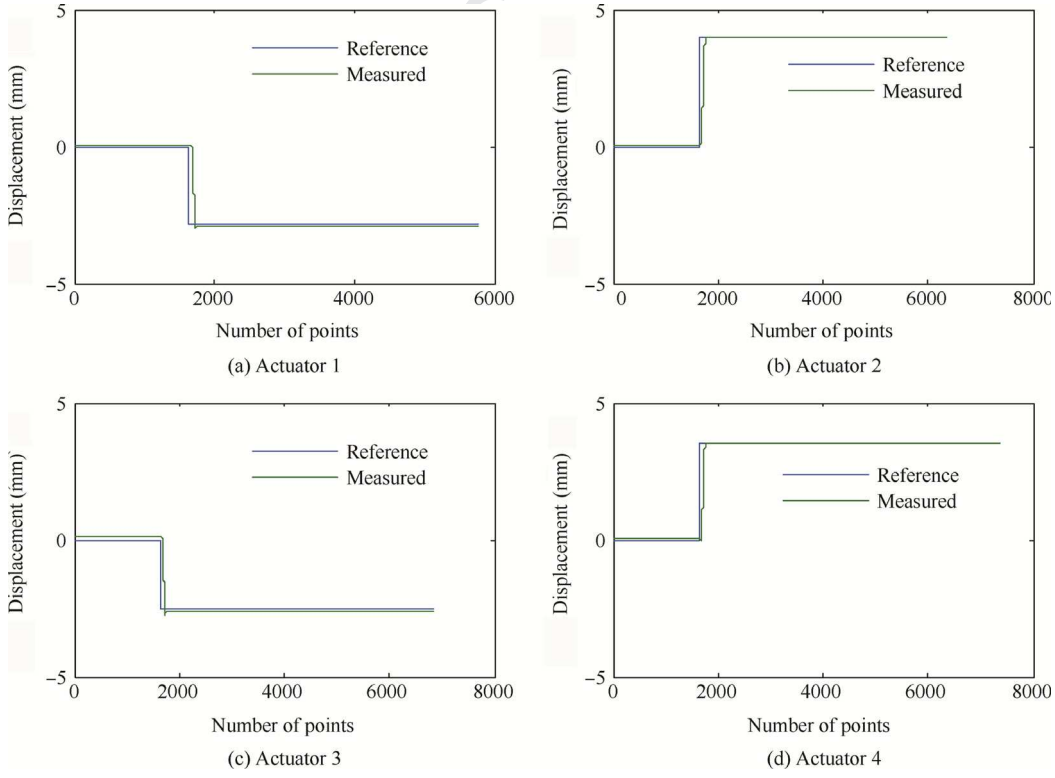

Fig. 9 Simultaneous actuation in four morphing wing points.

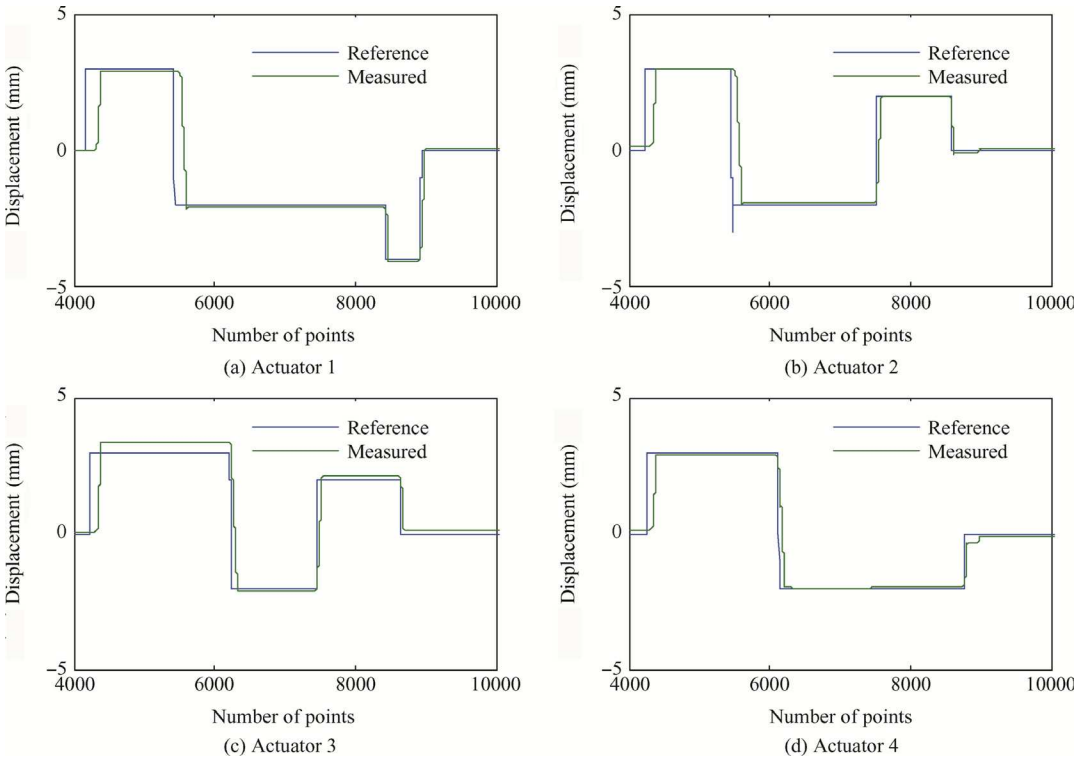

Fig. 10 Repeated step independent actuation in four morphing wing points.

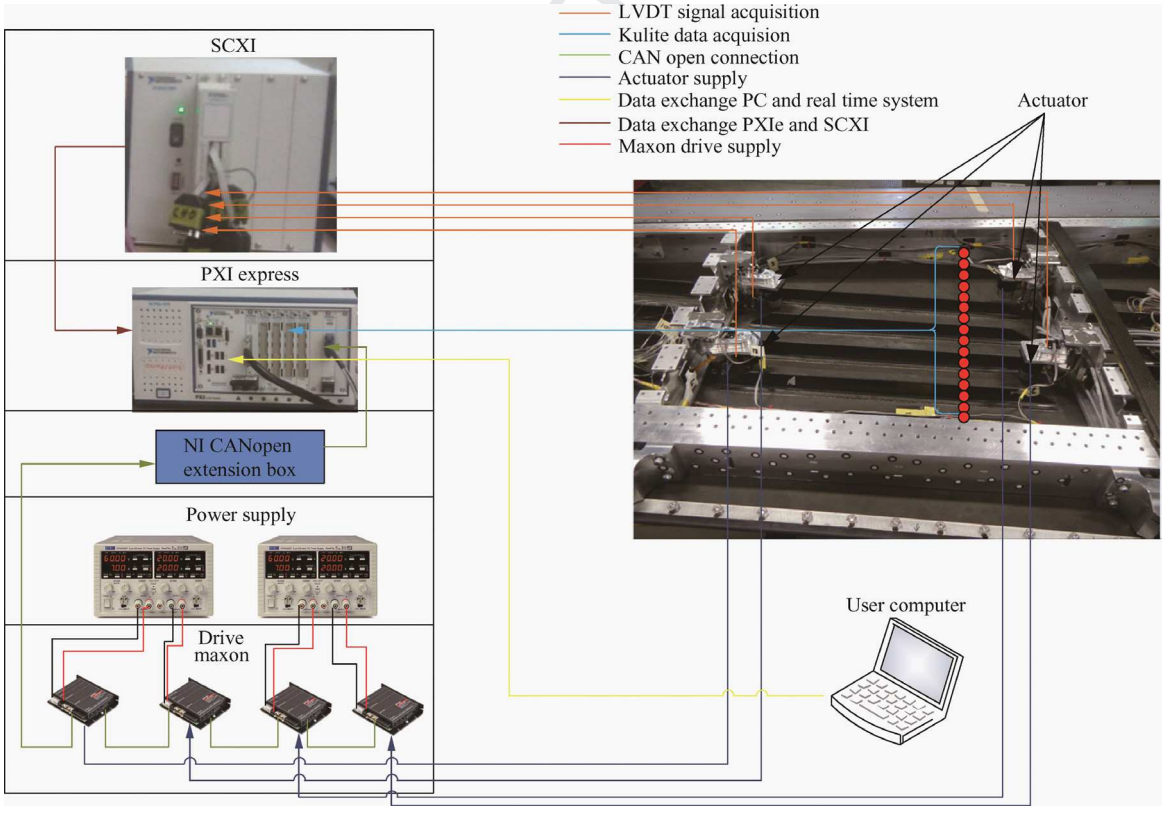

Fig. 11 Experimental setup in wind tunnel.

sor signal modules is able to process a maximum of 8 pressure sensors' signals, thereby covering all 32 of the used Kulite pressure sensors. The pressure data acquisition was performed at 20k samples/s for each channel. All pressure data were connected directly to the modular cards inserted inside the PXI-e chassis. All raw data for the 32 Kulite sensors were saved into the real-time system's hard drive for post-processing. The pressure coefficient curves obtained by calculating the dynamic pressure and by using the pressure Kulite data were displayed in real time for all the optimized flight cases. Signals from the LVDTs were also displayed for the different optimized flight cases. The end user selected the desired flight case from the GUI and the desired displacements were automatically loaded.

The data flow between the real-time controller and the computer is indicated by the double arrow line in yellow in Fig. 11, while the CAN open communication in the network is highlighted by the green arrow.

5. Wind tunnel test results

Wind tunnel test was performed at the IAR-NRC wind tunnel facility in Ottawa. During this first set of wind tunnel tests, 97 flight cases were tested: nineteen values for the angles of attack, three for the Mach numbers, and thirteen for the aileron deflection angles. The angles of attack values varied from $-3°$ to $+3°$, the Mach number values varied between 0.15 and 0.25, and the aileron deflection angles varied from $-6°$ to $+6°$. The ninety-seven desired optimized airfoils were obtained by changing the upper surface of the wing in the vertical direction. The aerodynamic goal was to extend the laminar region by moving the transition point as near as possible to the wing trailing edge with a constant lift.[53] Other publications are regarded as adaptive trailing-edge device research.[54,55] Various new genetic neural network methodologies were used for morphing wing control, modeling and identification, as well as for aircraft and helicopters.[56–60]

Thus, the wing model was tested in open loop architecture, the main signals such as the raw pressure signal data from the Kulite sensors, the skin displacements from linear positioning sensors, actuator current, and actuator speed were recorded. In this configuration, the loop was closed by using the LVDT signal as feedback for the controller. The pressure sensor signals were used to visualize the start of the transition in real time through power spectra analyses, while the calculated pressure coefficients were used to validate the aerodynamically predicted wing shapes. The real time acquired raw pressure signals were post-processed to obtain the FFT spectral decomposition, the standard deviation (STD) calculation, and the location of the transition. The raw pressure signals were filtered to remove parasitic noise.

The results obtained for an actuation case ($Ma = 0.25$, $\alpha = 0.5°$, $\delta = -1°$) are shown in Fig. 12. For all actuated cases, it was found that the controller performed well with the static error consistently less than 0.1 mm. The rise time was between 1 and 2 s, more than adequate for our morphing application. The measured positions for the four actuators were sensed by the LVDTs, while the desired positions were loaded from the database made from the data predicted by the aerodynamic team.

During the tests, the user's computer was installed in the control room of the wind tunnel facility, linked to the real-time system with an Ethernet cable. The four miniature actuators installed inside the wing and the aileron actuator were controlled via a new GUI developed by the research team especially for the wind tunnel tests. The GUI used to control the whole equipment during the wind tunnel tests is shown in Fig. 13. The graphical characteristics in Fig. 13 (orange frame) show the plots of the measured skin displacements and the reference skin displacements. The "emergency stop" push button deactivates the entire system and brings it back to its reference.

The "flight case selection" button loads the flight case number with its flight conditions (Mach number, aileron deflection angle and angle of attack), as it is shown in the blue frame of Fig. 13. Under "Mode selection", the user is able to select three different modes: Manual, Flight case and Homing. The "Homing" mode sends the system back to its reference state. The "Manual" mode allows the user to give skin position set points that are different than those of the database. The numerical controls ("Set point act 1", "Set point act 2", "Set point act 3" and "Set point act 4") are used for this purpose. Each actuator can be controlled individually in "Manual" mode by pushing one of the following buttons: "Activate act 1", "Activate act 2", "Activate act 3", "Activate act 4", or they can be moved simultaneously after pushing the "Act_all_manual" button. The numerical values for the skin displacements as well as the real skin displacements are displayed using the numerical indicators shown in Fig. 13 (white frame). In "Flight case" mode, when a flight case is selected and the flight conditions have been loaded, the user has to activate the controller by changing the value of the numerical control buttons "Activated act 1 & 3" and "Activated act 2 & 4" to 1.

Kulite pressure sensors are used to capture what happens over the flexible skin when the wind is blowing. They are very sensitive, highly accurate differential sensors, and the pass band of their values is logged for each flight case. The log file is created once the "Logging Enabled" button is pressed, and the logging starts immediately. The logging stops when the button is released. The same procedure is used for the logging of the numerical values of the LVDTs and motor data such as velocity, encoder and current.

An aileron is attached to the experimental wing; its position is controlled by means of an electromechanical actuator. The red frame in Fig. 13 indicates how all the information to control the aileron actuator is collected. The aileron drive status is given by the radio button "DRIVSTAT", where the actual aileron actuator position in degrees is displayed on the numerical indicator "Aileron_angle", while the motion task to send to the drive is inputted by selecting "Motion task" from the menu "operation".

The 32 Kulite pressure sensors are installed on the upper surface to sense the static pressure on the wing. They are located between 28% of the chord and 68% of the chord. To evaluate the aerodynamic gain of the morphing wing technology on the experimental model, the recorded pressure data during the wind tunnel tests were post-processed in order to obtain the pressure coefficient distribution curve and the spectral repartition of the pressure. The transition region determined by the flow separation and characterized by the amplification of the Tollmien-Schlichting waves was captured by the Kulite pressure sensors. The same aerodynamic gain was also evaluated by using the infrared thermography technique. The pressure data were recorded at 20 kHz rate for both

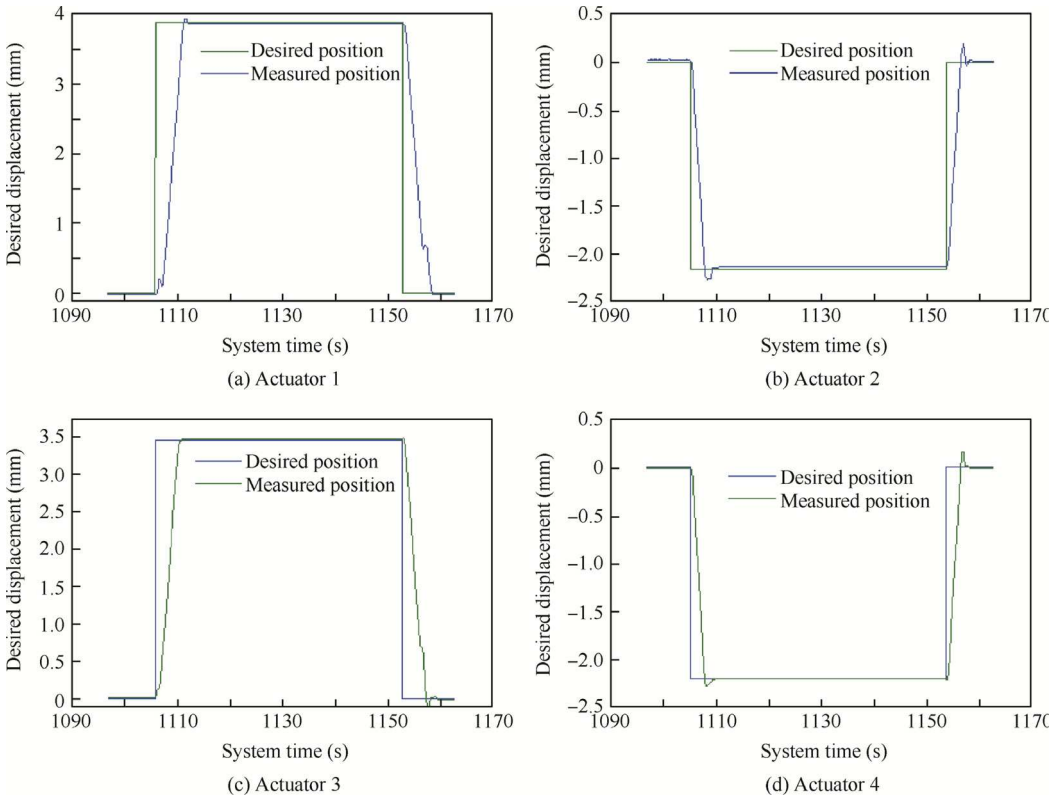

Fig. 12 Wind tunnel controller results for flight case 38 ($Ma = 0.25$, $\alpha = 0.5°$, $\delta = -1°$).

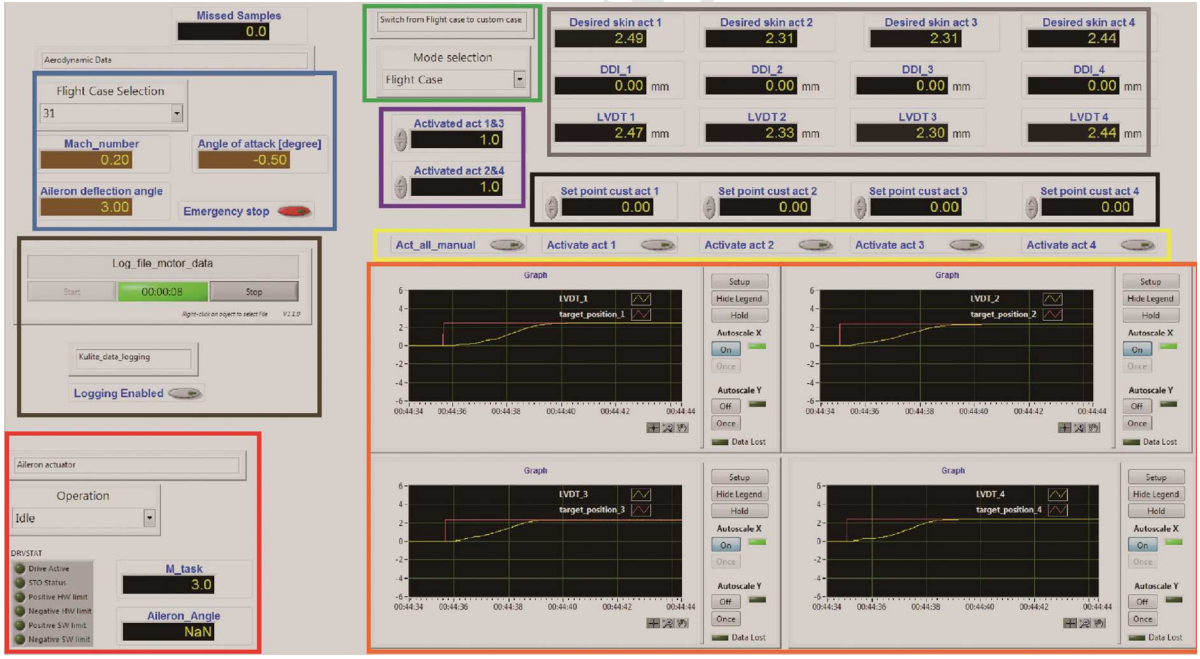

Fig. 13 GUI for wind tunnel tests.

un-morphed and morphed airfoils in ninety-seven flow cases, and were analysed using FFT decomposition to detect the magnitude of the noise in the surface air flow. Subsequently, the data were high pass filtered at 1 kHz and processed by calculating the STD of the signal to obtain a plot diagram of the pressure fluctuations in the flow boundary layer.

A higher standard deviation detected by a Kulite array sensor suggests that the sensed pressure signal is affected by

turbulence which started somewhere between this sensor and the previous sensor. Similar effects can be observed at the level of the FFT evaluated for all pressure sensors, a detached FFT curve suggesting a turbulent flow over the respective pressure sensor. The resolution of the laminar to turbulent transition point position establishment is directly influenced by the density of the pressure sensors evaluating the flow characteristics.

For the flow case 70 associated to $Ma = 0.2$, $\alpha = 1°$, $\delta = 4°$, Fig. 14 presents the STDs of the acquired pressure data both for un-morphed and morphed airfoils. The results show that the transition for un-morphed airfoil begins on the pressure sensors #6 and #7, while for morphed airfoil it begins on the sensor #15. On the other way, the maximum value of the STD for un-morphed airfoil was associated with the sensor #13, while that for morphed airfoil was associated with the sensor #19.

Figs. 15 and 16 depict the FFT evaluation results for un-morphed airfoil and morphed airfoil in the conditions established by the flow case 70 ($Ma = 0.2$, $\alpha = 1°$, $\delta = 4°$), respectively. For a better visualization of the transition location, the 32 Kulite sensors' FFTs were represented in four independent windows in groups of eight consecutive sensors starting from the leading edge. Figures also provide a centralized representation of the FFTs for all 32 sensors for the easiest observation of the FFT curves detachment.

The FFT associated to the un-morphed airfoil shows that the curve corresponding to the sensor #6 is easiest detached, indicating the transition beginning. A more visible detachment appears at the level of the sensors #12 and #13, producing the transition to the upper FFT curves package. For the morphed airfoil, the FFT characteristics show that the transition begins on the sensor #15, the maximum influenced FFT curves corresponding to the sensor #19. As a consequence, the FFT and STD based conclusions are similar for this flow case, the laminar region being extended with over 4% of the chord in the Kulite sensor section.

For capturing the transition region over the entire wing model surface infrared (IR) thermography camera visualizations were performed. The wing leading edge, its upper surface flexible skin and the aileron interface were coated with high emissivity black paint to improve the quality of the IR photographs. The span-wise stations, where the two pressure sensors lines were installed were not painted, in order to not influence the pressure reading quality. A Jenoptik Variocam camera, with a resolution of 640×480 pixels, was used to measure the surface temperatures. This camera was equipped with 60° lens in order to capture the flow transition on the entire upper surface of the wing. Wind tunnel experimental test was conducted for all the aerodynamic optimized cases.

The infrared (IR) image of the whole wing during wind tunnel test for flight case 70 is shown in Fig. 17, Fig. 17(a) is un-morphed/reference airfoil, Fig. 17(b) is morphed airfoil. The IR technique makes it possible to visualize and estimate online the transition location on the wing. The red frame indicates the limits of the flexible skin, which is made of composite materials. The line of Kulite sensors and the spots showing the four actuators are visible as well. The black line indicates the estimated transition line, and the white lines indicate the tolerance band. The thermography methodology (infrared methodology) is based on the temperature gradient in the laminar and turbulent flow. The blue region inside the red frame in Fig. 17 indicates the laminar region (low temperature region) while the yellow color inside the same frame shows the turbulent region (high temperature region). The wind is blowing from left to right. According to the IR transition images given by Fig. 17 for $Ma = 0.2$, $\alpha = 1°$, $\delta = 4°$, the transition has been delayed by about 4%. With no actuation, the transition was located at about 48% of the chord (Fig. 17(a)), while with actuation, the transition located closer to the trailing edge, thus, at 52% of the chord. In addition, a very good match was obtained between the IR imaging and the Kulite sensors in terms of the transition location.

6. Conclusions

This paper has presented results obtained in a new morphing wing project, as part of the development and experimental test of a variant of the control system used in the actuation of the flexible skin on a wing upper surface. In the exposed control architecture, called generically "open loop", the morphing wing shapes and the aileron deflection angles were controlled. The designed control system was tested experimentally in bench tests with no aerodynamic load, and then, in wind tunnel tests, with aerodynamic load(s). Proportional fuzzy feed-forward architecture was chosen for controlling the actuation lines. The "open loop" architecture of the control system was based on a database with the optimized airfoils, obtained as a result of a preliminary aerodynamic numerical optimiza-

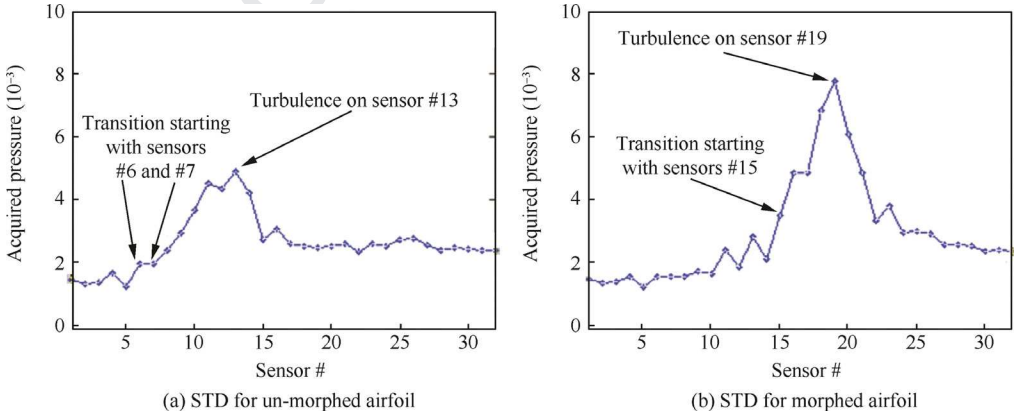

Fig. 14 STD of pressure data acquired for $Ma = 0.2$, $\alpha = 1°$, $\delta = 4°$ flow case.

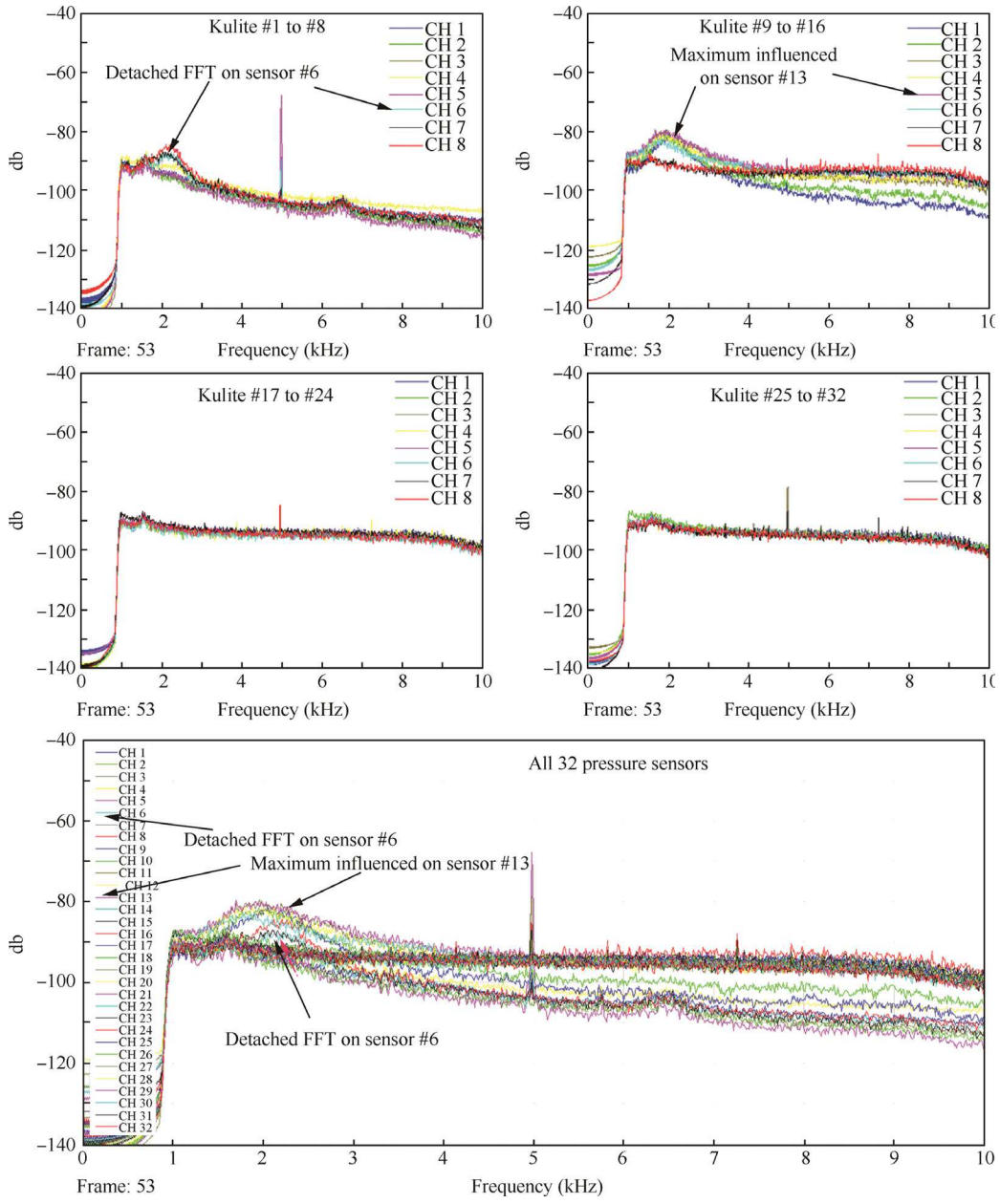

Fig. 15 FFT results for unmorphed airfoil in flow case 70 (Ma = 0.2, α = 1°, δ = 4°).

tion, applied for several flight cases as combinations of Mach numbers Ma, angles of attack α and aileron deflection angles δ. The database was firstly used to validate the morphing concept on this wing model for several flight cases covering a flight envelope, and subsequently, it may be used as "validated database of optimized airfoils" to generate another "optimized airfoils" through interpolation in the development of the embedded control system for a "real morphing wing" boarded on an aircraft, having as inputs the Mach number, the angle of attack and the aileron deflection angle provided by the onboard equipment.

The first testing phase, the bench test, also allowed the evaluation of the level of reproducibility of the numerically optimized shape of the upper surface of the wing with the experimentally obtained one. In this way, the morphed wing was laser-scanned for each optimized airfoil in the database, and software results were compared with the numerical results. The bench test results were very good, validating the experimental model for the next testing level with aerodynamic loads conducted in the IAR-NRC wind tunnel in Ottawa. During the test of all the optimized flight cases, the values of the static errors were under the limit established by the aerodynamics, i.e. 0.1 mm; from the numerical simulations, the aerodynamic team observed that in a range between −0.1 mm and 0.1 mm around the optimized position the estimated transition point position of the upper surface flow is approximately the same.

The second testing phase, the wind tunnel test, allowed the validation of the aerodynamic optimization of the system through the visualization of the transition point position for each optimized airfoil in the database (for all optimized flight

Please cite this article in press as: Kammegne MJT et al. Proportional fuzzy feed-forward architecture control validation by wind tunnel tests of a morphing wing, *Chin J Aeronaut* (2017), http://dx.doi.org/10.1016/j.cja.2017.02.001

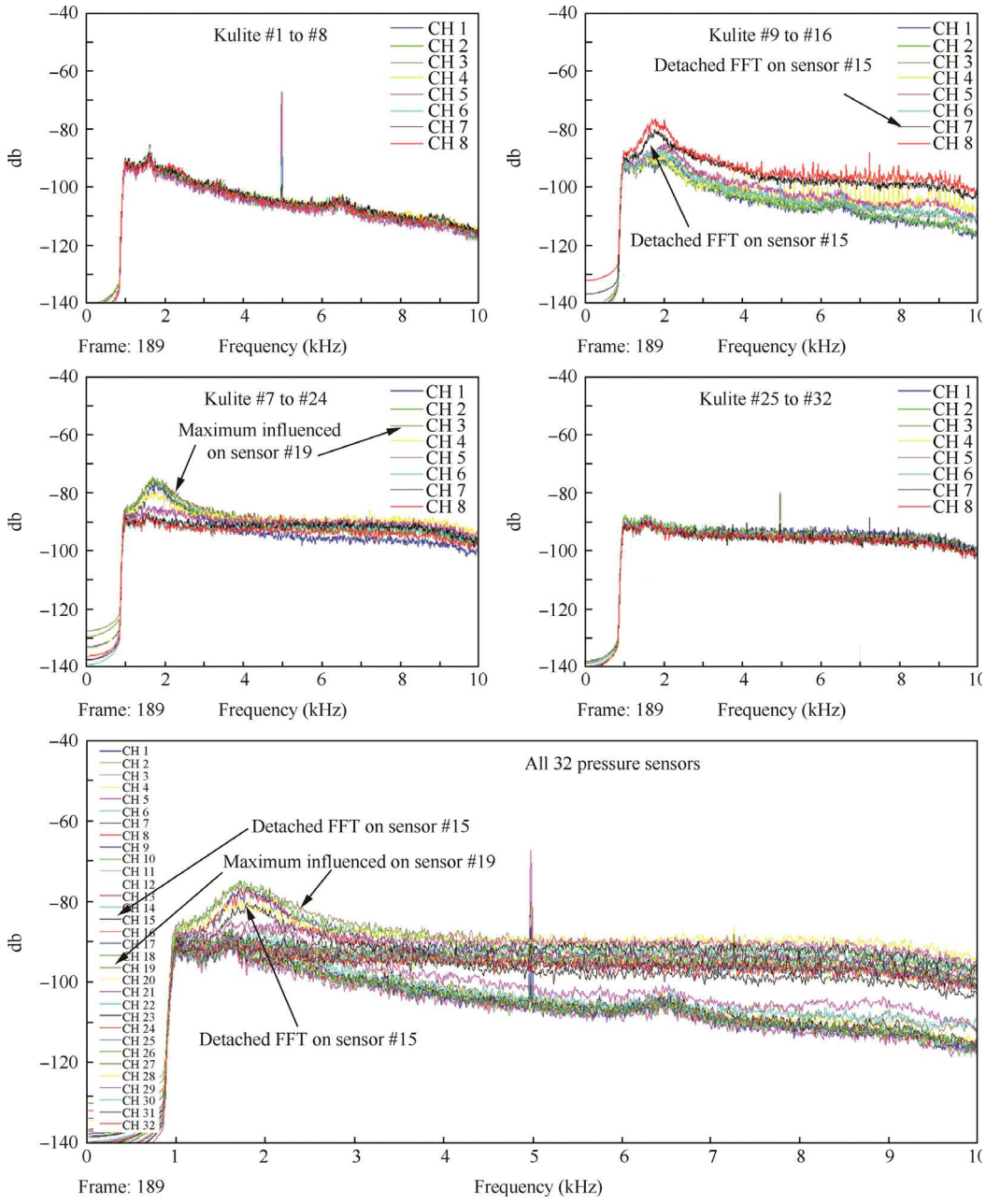

Fig. 16 FFT results for morphed airfoil in flow case 70 ($Ma = 0.2$, $\alpha = 1°$, $\delta = 4°$).

cases) based on the information provided by 32 Kulite pressure sensors installed on the flexible skin. The IAR-NRC experimental facility allowed for a supplementary evaluation method for the transition point position in wind tunnel tests, the IR visualization of the flow. The recorded pressure data during the wind tunnel tests were post-processed in order to obtain the pressure coefficient distribution curve and the spectral repartition of the pressure. The transition region determined by the flow separation and characterized by the amplification of the Tollmien-Schlichting waves was captured by the Kulite pressure sensors. The pressure data were recorded at 20 kHz rate for both un-morphed and morphed airfoils in ninety-seven flow cases, and were analysed using FFT decomposition to detect the magnitude of the noise in the surface air flow. Subsequently, the data were high pass filtered at 1 kHz and processed by calculating the STD of the signal to obtain a plot diagram of the pressure fluctuations in the flow boundary layer. Similar to the bench tests, for all actuated cases it was found that the controller performed well, with static error consistently being less than 0.1 mm.

The wind tunnel testing results exposed in the paper and obtained with the FFT, STD and IR evaluations for the flight case 70 ($Ma = 0.2$, $\alpha = 1°$, $\delta = 4°$) have shown that the transition was delayed by about 4%, from close to 48% of the chord in the un-morphed situation to 52% of the chord in the morphed situation. In addition, a good match was obtained between the IR and Kulite pressure sensors' results in terms of the transition location.

Please cite this article in press as: Kammegne MJT et al. Proportional fuzzy feed-forward architecture control validation by wind tunnel tests of a morphing wing, *Chin J Aeronaut* (2017), http://dx.doi.org/10.1016/j.cja.2017.02.001

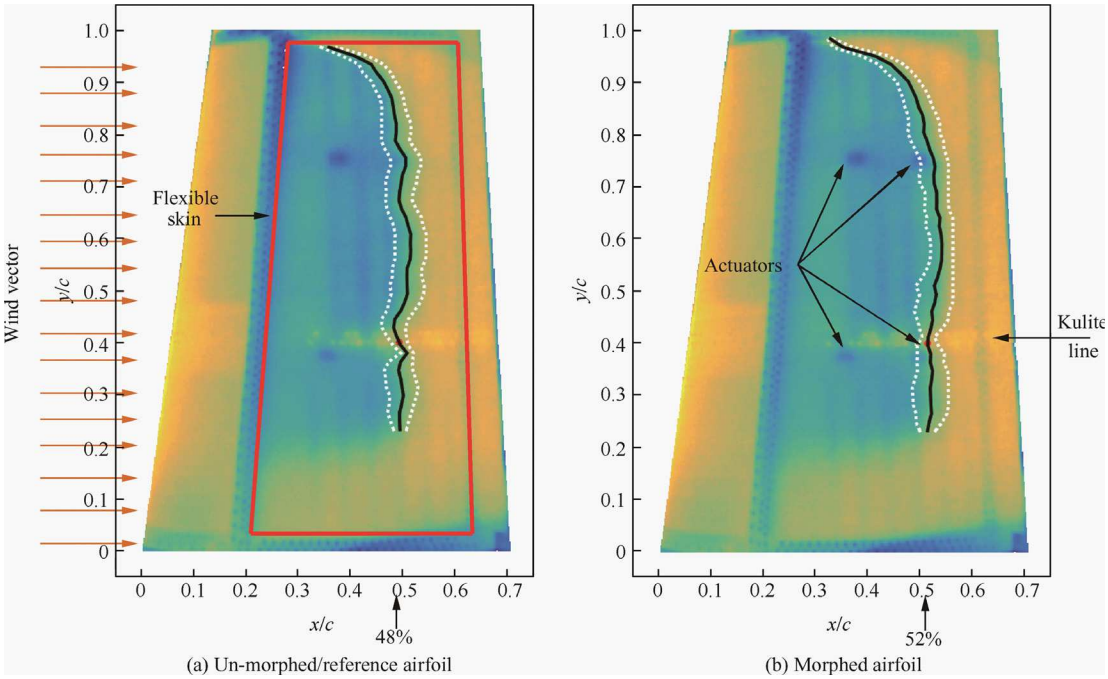

Fig. 17 Infrared image capture for flight case 70 ($Ma = 0.2$, $\alpha = 1°$, $\delta = 4°$).

On the other hand, the experimentally obtained results for all tested flight cases confirmed the feasibility of the morphing wing technology. Given that our project used a real wing structure, we create the premises for a future application of this technology to real aircrafts.

Acknowledgments

The authors would like to thank the Thales Avionics team for their support, especially Mr. Philippe Molaret, Mr. Bernard Bloiuin and Mr. Xavier Louis, as well as the Bombardier Aerospace team, Mr. Patrick Germain and Mr. Fassi Kafyeke in particular. We would also like to thank the Consortium for Research and Innovation in Aerospace in Quebec (CRIAQ) and the National Sciences and Engineering Research Council (NSERC) for their funding of the CRIAQ MDO 505 project. Thanks are also due to Master student Yvan Tondji for his help in data post-processing.

References

1. Sofla AYN, Meguid SA, Tan KT, Yeo WK. Shape morphing of aircraft wing: status and challenges. *Mater Des* 2010;**31**(3):1284–92.
2. Zingg DW, Diosady L, Billing L. Adaptive airfoils for drag reduction at transonic speeds*24th AIAA applied aerodynamics conference*. Reston: AIAA; 2006.
3. Friswell MI. The prospects for morphing aircraft. IV ECCOMAS thematic conference on smart structures and materials; 2009.
4. Rodriguez AR. Morphing aircraft technology survey*45th AIAA aerospace sciences meeting and exhibit*. Reston: AIAA; 2007.
5. Weisshaar T. Morphing aircraft technology-new shape for aircraft design. Multifunctional structures/integration of sensor and antennas meeting. O1-1-20.
6. Barbarino S, Bilgen O, Ajaj RM, Friswell MI, Inman DJ. A review of morphing aircraft. *J Intell Mater Syst Struct* 2011;**22**(9):823–77.
7. Prock BC, Weisshaar TA, Crossley WA. Morphing airfoil shape change optimization with minimum actuator energy as an objective*9th AIAA/ISSMO symposium on multidisciplinary analysis and optimization*. Reston: AIAA; 2002.
8. Pern N, Jacob J. Aerodynamic flow control using shape adaptive surfaces*ASME design engineering technical conferences*. New York: ASME; 1999.
9. Hiroharu S, Kenichi R, Asei T. Laminar airfoil modification attaining optimum drag reduction by use of airfoil morphing. *J Aircaft* 2010;**47**(4):1126–32.
10. Schroder W, Meijering A. Transonic flow over an adaptive wing section. *GAMM-Mitteilungen* 2005;**28**(1):56–72.
11. Munday D, Jacob J. *Low speed morphing wing flow control*. Kentucky: University of Kentucky Press; 2001.
12. Munday D, Jacob J. Active control of separation on a wing with conformal camber*39th AIAA aerospace sciences meeting and exhibit*. Reston: AIAA; 2001.
13. Munday D, Jacob J. Active control of separation on a wing with oscillating camber. *AIAA J Aircaft* 2002;**39**(1):187–9.
14. Lebeau R, Karam A, Pern N, Jacob J. Analysis of low speed flow over an adaptive airfoil with oscillating camber*48th AIAA aerospace sciences meeting including the new horizons forum and aerospace exposition*. Reston: AIAA; 2010.
15. Miller SJ. *Adaptive wing structures for aeroelastic drag reduction and loads alleviation [dissertation]*. Manchester: University of Manchester; 2010.
16. Monner HP, Hanselka H, Breitbach E. Development and design of flexible Fowler flaps for an adaptive wing. In: SPIE's 5th annual international symposium on smart structures and materials; 1998. p. 60–70.
17. Poonsong P. *Design and analysis of a multi-section variable camber wing [dissertation]*. Washington, D.C.: University of Maryland; 2004.
18. Saggere L, Kota S. Static shape control of smart structures using compliant mechanisms. *AIAA J* 2009;**37**(5):572–8.
19. Kota S, Osborn R, Ervin G, Maric D, Flick P, Paul D. Mission adaptive compliant wing – design, fabrication and flight test. In: RTO applied vehicle technology panel (AVT) symposium; 2009.

20. Baker D, Friswell MI. The design of morphing aerofoils using compliant mechanisms. In: 19th International conference on adaptive structures and technologies; 2008.
21. Campanile LF, Sachau D. The belt-rib concept: a structronic approach to variable camber. *J Intell Mater Syst Struct* 2000;**11**(3):215–24.
22. Wang DP, Bartley-Cho JD, Martin CA, Hallam BJ. Development of high-rate large-deflection hingeless trailing-edge control surface for the smart wing wind tunnel model*SPIE, smart structures and materials 2001: industrial and commercial applications of smart structures technologies*. Washington, D.C.: SPIE; 2001.
23. Vos R, Barrett R, Breuker Rd, Tiso P. Post-buckled precompressed elements: a new class of control actuators for morphing wing UAVs. *Smart Mater Struct* 2007;**16**(3):919–26.
24. Lim SM, Lee S, Park HC, Yoon KJ, Goo NS. Design and demonstration of a biomimetic wing section using a lightweight piezo-composite actuator (LIPCA). *Smart Mater Struct* 2005;**14**(4):496–503.
25. Heryawan Y, Park HC, Goo NS, Yoon KJ, Byun YH. Design and demonstration of a small expandable morphing wing*Smart structures and materials 2005: smart structures and integrated systems*. Washington, D.C.: SPIE; 2005. p. 224–31.
26. Ray CW, Batten BA, Singler JR. A model based feedback controller for wing-twist via piezoceramic actuation*American control conference*. Piscataway (NJ): IEEE Press; 2011. p. 2362–7.
27. Ray CW, Batten BA, Singler JR. Feedback control of a bioinspired plate-beam system*49th IEEE conference on decision and control (CDC)*. Piscataway (NJ): IEEE Press; 2010. p. 1719–24.
28. Usher TD, Ulibarri KR, Camargo GS. Piezoelectric microfiber composite actuators for morphing wings. *ISRN Mater Sci* 2013;**2013**(1):1–8.
29. Bilgen O, Kochersberger KB, Inman DJ. Macro-fiber composite actuators for a swept wing unmanned aircraft. *Aeronautical J – New Series* 2009;**113**(1144):385–95.
30. Bilgen O, Kochersberger KB, Inman DJ, Ohanian OJ. Macro-fiber composite actuated simply supported thin airfoils. *Smart Mater. Struct.* 2010;**19**(5):055010.
31. Bilgen O, Friswell MI, Kochersberger KB, Inman DJ. Surface actuated variable-camber and variable-twist morphing wings using piezocomposites. Reston: AIAA; 2011. Report No.: AIAA-2011-2072.
32. Na YH, Kim JH. Smart wing using piezoelectric actuators. In: IMAC-XXIV: conference & exposition on structural dynamics; 2006.
33. Barbarino S, Pecora R, Lecce L, Concilio A, Ameduri S, Calvi E. A novel SMA-based concept for airfoil structural morphing. *J Mater Eng Perform* 2009;**18**(5):696–705.
34. Seow AK, Liu Y, Yeo WK. Shape memory alloy as actuator to deflect a wing flap. Reston: AIAA; 2008. Report No.: AIAA-2008-1704.
35. Giuseppe M. Design and demonstrators testing of adaptive airfoils and hingeless wings actuated by shape memory alloy wires. *Smart Struct Syst* 2007;**3**(1):89–114.
36. Abdullah EJ, Bil C, Watkins S. Application of smart materials for adaptive airfoil control. Reston: AIAA; 2009. Report No.: AIAA-2009-1359.
37. Abdullah EJ, Bil C, Watkins S. Numerical simulation of an adaptive airfoil system using SMA actuators. Reston: AIAA; 2010. Report No.: AIAA-2010-1209.
38. Popov AV, Botez RM, Labib M. Transition point detection from the surface pressure distribution for controller design. *J Aircraft* 2008;**45**(1):23–8.
39. Grigorie TL, Botez RM, Popov AV. Adaptive neuro-fuzzy controllers for an open loop morphing wing system. *Proc Inst Mech Eng, Part G: J Aerospace Eng* 2009;**223**(7):965–75.
40. Grigorie TL, Popov AV, Botez RM, Mamou M, Mébarki Y. On–off and proportional-integral controller for a morphing wing. Part 1: Actuation mechanism and control design. *Proc Inst Mech Eng, Part G: J Aerospace Eng* 2011;**226**(2):131–45.
41. Grigorie TL, Popov AV, Botez RM, Mamou M, Mébarki Y. On–off and proportional–integral controller for a morphing wing. Part 2: Control validation–numerical simulations and experimental tests. *Proc Inst Mech Eng, Part G: J Aerospace Eng* 2011;**226**(2):146–62.
42. Grigorie TL, Popov AV, Botez RM, Mamou M, Mébarki Y. A hybrid fuzzy logic proportional-integral-derivative and conventional on-off controller for morphing wing actuation using shape memory alloy. Part 1: Morphing system mechanisms and controller architecture design. *Aeronaut J* 2012;**116**(1179):433–49.
43. Grigorie TL, Popov AV, Botez RM, Mamou M, Mébarki Y. A hybrid fuzzy logic proportional-integral-derivative and conventional on-off controller for morphing wing actuation using shape memory alloy. Part 2: Controller implementation and validation. *Aeronaut J* 2012;**116**(1179):451–65.
44. Popov AV, Grigorie TL, Botez RM, Mamou M, Mébarki Y. Real time morphing wing optimization validation using wind-tunnel tests. *J Aircraft* 2010;**47**(4):1346–55.
45. Popov AV, Grigorie TL, Botez RM, Mamou M, Mébarki Y. Closed-loop control validation of a morphing wing using wind tunnel tests. *J Aircraft* 2010;**47**(4):1309–17.
46. Kammegne MJT, Grigorie TL, Botez RM, Koreanschi A. Design and validation of a position controller in the Price-Païdoussis wind tunnel. In: Proceeding of the IASTED modelling, simulation and control conference; 2014.
47. Sugar Gabor O, Koreanschi A, Botez RM. Low-speed aerodynamic characteristics improvement of ATR 42 airfoil using a morphing wing approach*IECON 38th annual conference on IEEE industrial electronics society*. Piscataway (NJ): IEEE Press; 2012. p. 5451–6.
48. Koreanschi A, SugarGabor O, Botez RM. Numerical and experimental validation of a morphed wing geometry using Price-Païdoussis wind tunnel testing. Reston: AIAA; 2015. Report No.: AIAA-2015-3386.
49. Tchatchueng Kammegne MJ, Grigorie TL, Botez RM, Koreanschi A. Design and wind tunnel experimental validation of a controlled new rotary actuation system for a morphing wing application. *Proc Inst Mech Eng, Part G: J Aerospace Eng* 2016;**230**(1):132–45.
50. Hassig A, Brossard J, Botez R. Calibration issues in the subsonic Price – Paidoussis wind tunnel. In: CASI AÉRO 2013 conference, 60th aeronautics conference and AGM; 2013.
51. Kovacic Z, Bogdan S. *Fuzzy controller design – theory and applications*. Taylor and Francis Group; 2006.
52. Hampel R, Wagenknecht M, Chaker N. *Fuzzy control—theory and practice*. Berlin Heidelberg: Springer; 2000.
53. Koreanschi A, Gabor Sugar O, Botez RM. Boundary layer behavior on morphing upper surface wings with shape changing aileron – new analysis techniques. Reston: AIAA; 2014. Report No.: AIAA-2014-3170.
54. Diodati G, Concilio A, Ricc S, DeGaspari A, Liauzun C, Godard JL. Estimated performance of an adaptive trailing-edge device aimed at reducing fuel consumption on a medium-size aircraft. *Proc SPIE – Int Soc Opt Eng* 2013;**8690**(1):158–66.
55. Ameduri S, Concilio A, Pecora R. A SMA-based morphing flap conceptual and advanced design. *Smart Struct Syst* 2015;**16**(3):555–77.
56. Mosbah AB, Botez RM, Dao TM. Hybrid original approach for the prediction of the aerodynamic coefficients of an ATR-42 scaled wing model. *Chin Aeronautical J* 2016;**29**(1):41–52.
57. Ren Y, Bai GC. New neural network response surface methods for reliability analysis. *Chin J Aeronaut* 2011;**24**(1):25–31.

58. Roudbari A, Saghafi F. Intelligent modeling and identification of aircraft nonlinear flight. *Chin J Aeronaut* 2014;**27**(4):759–71.
59. Lu XL, Liu H, Wang GL, Wu Z. Helicopter sizing based on genetic algorithm optimized neural network. *Chin J Aeronaut* 2016;**19**(3):212–8.
60. Xu YM, Li S, Rong XM. Composite structural optimization by genetic algorithm and neural network response surface modeling. *Chin J Aeronaut* 2005;**18**(4):301–16.

Please cite this article in press as: Kammegne MJT et al. Proportional fuzzy feed-forward architecture control validation by wind tunnel tests of a morphing wing, *Chin J Aeronaut* (2017), http://dx.doi.org/10.1016/j.cja.2017.02.001